MusE gas flow and wind (MEGAFLOW) VI: a study of C IV and Mg II absorbing gas surrounding [O II] emitting galaxies

Schroetter, I.; Bouché, N.F.; Zabl, J.; Rahmani, H.; Wendt, M.; Muzahid, S.; ... ; Wisotzki, L.

MNRAS 000, 1–8 (0000) Preprint November 21, 2021 Compiled using MNRAS LATEX style file v3.0

MusE GAs Flow and Wind (MEGAFLOW) VI. A study of C IV and Mg II absorbing gas surrounding [O II] emitting galaxies ⋆

Ilane Schroetter,[1,5]† Nicolas F. Bouché,[2] Johannes Zabl,[2] Hadi Rahmani,[1,7] Martin Wendt,[3,4] Sowgat Muzahid,[4] Thierry Contini,[5] Joop Schaye,[6] Kasper B. Schmidt,[4] Lutz Wisotzki [4]

[1] GEPI, Observatoire de Paris, PSL Université, CNRS, 5 Place Jules Janssen, 92190 Meudon, France
[2] Univ Lyon, Univ Lyon1, Ens de Lyon, CNRS, Centre de Recherche Astrophysique de Lyon UMR5574, F-69230 Saint-Genis-Laval, France
[3] Institut für Physik und Astronomie, Universität Potsdam, Karl-Liebknecht-Str. 24/25, 14476 Golm, Germany
[4] Leibniz-Institut für Astrophysik Potsdam, An der Sternwarte 16, D-14482 Potsdam, Germany
[5] Institut de Recherche en Astrophysique et Planétologie (IRAP), Université de Toulouse, CNRS, UPS, F-31400 Toulouse, France
[6] Leiden Observatory, Leiden University, PO Box 9513, 2300 RA Leiden, The Netherlands
[7] School of Astronomy, Institute for Research in Fundamental Sciences (IPM), PO Box 19395-5531 Tehran, Iran

November 21, 2021

ABSTRACT

Using the MEGAFLOW survey, which consists of a combination of MUSE and UVES observations of 22 quasar fields selected to contain strong Mg II absorbers, we measure covering fractions of C IV and Mg II as a function of impact parameter b using a novel Bayesian logistic regression method on unbinned data, appropriate for small samples. In the MUSE data, we found 215 $z = 1 - 1.5$ [O II] emitters with fluxes $> 10^{-17}$ erg s^{-1} cm^{-2} and within 250 kpc of quasar sight-lines. Over this redshift path $z = 1 - 1.5$, we have 19 (32) C IV (Mg II) absorption systems with rest-frame equivalent width (REW) W_r >0.05Å associated with at least one [O II] emitter. The covering fractions of C IV (Mg II) absorbers with mean W_r ≈0.7Å (1.0Å), exceeds 50% within 30 (45) kpc, with a mild redshift evolution, in agreement with larger studies. For absorption systems that have C IV but not Mg II, we find in 80% of the cases no [O II] counterpart. This may indicate that the C IV, in these cases, come from the intergalactic medium (IGM), i.e. beyond 250 kpc, or that it is associated with lower-mass or quiescent galaxies.

Key words: galaxies: evolution — galaxies: formation — galaxies: intergalactic medium — quasars: absorption lines

1 INTRODUCTION

The surroundings of galaxies, the intergalactic medium (IGM) or the very close environment around galaxies: the circum-galactic medium (CGM), are known to be filled with gas in various phases. This gas can be either ionized or neutral. For instance, Mg II is probing the T∼ 10^4 K temperature gas whereas C IV probes T∼ 10^5K gas (see the CGM review of Tumlinson et al. 2017). Because the gas usually has low density compared to the gas in galaxies, it is very difficult to observe directly. Understanding the origin of the gas surrounding galaxies is one of the keys to drawing a precise picture of how galaxies form and evolve.

In order to study the structure of the gas surrounding galaxies, the covering fraction (fc) as a function of impact parameter is usually used. In order to study this fc, Mg II ($\lambda\lambda$2796, 2803) is a useful doublet its rest wavelengths make it easily detected in large surveys like Nielsen et al. (2013b) or Lan (2020). Another line which can be used to probe the surrounding gas of galaxies is C IV ($\lambda\lambda$1548, 1550). Indeed, this doublet, like Mg II is often detected if the wavelength coverage permits it. However, there are only few studies that constrain fc for this warm gas as a function of impact parameter. As an example, Prochaska et al. (2014) used quasar pairs from the Sloan Digital Sky Survey (SDSS) and found two bins of impact parameters up to 100 kpc from the host quasar. Landoni et al. (2016) added a few quasar pairs to the previous study as well as fc for Mg II and found that at a given impact parameter, Mg II tends to have a larger fc than C IV, meaning that C IV may be more patchy around galaxies than Mg II.

The origin of this highly ionized gas, C IV, and its distribution around galaxies, is thus still discussed. For example: Chen et al. (2001) found that C IV is extended, its envelopes goes up to a radius of ∼ 100 kpc around galaxies and that C IV absorbing strength scales with B-band luminosity. In their study, they used faint galaxies at impact parameters 10.9 < b < 1576 kpc in quasar (QSO)

⋆ Based on observations made with ESO Telescopes at the La Silla Paranal Observatory under programme IDs 094.A-0211, 095.A-0365, 096.A-0609, 096.A-0164, 097.A-0138, 097.A-0144, 098.A-0216, 098.A-0310, 099.A-0059, 293.A-5038

† E-mail: ilane.schroetter@obspm.fr

fields using HST. Those galaxies have redshifts $z < 1.2$ and they detected 36 C IV absorbers in 24 QSO fields. They also argued that C IV is not likely to come from outflows (which, in their study, are believed to extend up to 20 kpc) but is rather stripped from satellites around each galaxy. Rauch et al. (2001) observed 3 lensed QSO fields with Keck HIRES spectrograph. They found 34 C IV absorbers with redshifts $z < 3.62$ and concluded that C IV must be located outside of the host galaxy. Schaye et al. (2003) detected widespread C IV absorption associated with H I absorption at $z \approx 3$. The study of Fox et al. (2007), in which they analysed 81 Damped Lyman Alpha (DLA) and sub-DLA systems with UVES at redshift $1.9 < z < 3.6$ found 63 (DLA) + 11(sub-DLA) C IV absorbers. They found that star formation and supernovae (SNe) can provide enough energy to heat and accelerate C IV clouds. This could explain the highest C IV component velocity above the escape velocity. Fox & Richter (2016) show one case of outflow with redshifted C IV absorption at $z \approx 2$. Du et al. (2016), using 96 DEEP2 galaxies at redshifts $z \approx 1$, detected C IV absorption around 32 out of 46 galaxies and concluded that C IV and Mg II velocities are nearly identical. In their study, they also found that the gas velocity and the Equivalent width (EW) of C IV correlate with the star formation rate (SFR) and the specific SFR (sSFR) of the host galaxy. Turner et al. (2014) found widespread C IV out to 100 kpc around $z \approx 2$ star-forming galaxies. They also detected strong redshift space distortions. Turner et al. (2017) concluded from a comparison to the EAGLE simulation (Schaye et al. 2015) that the C IV mainly comes from inflows. All those studies show a clear lack of consensus on the origin and properties of this highly ionized gas. However, they agree that the gas is mainly located outside their host galaxies and has similarities with Mg II properties.

In this paper, we aim to use our novel Bayesian logistic method on unbinned data to address the question of how C IV is located around galaxies compared to Mg II by searching for C IV absorption systems and their possible galaxy counterparts and by studying the C IV and Mg II covering fractions using the MEGAFLOW survey (Schroetter et al. 2016; Zabl et al. 2019; Schroetter et al. 2019; Zabl et al. 2020).

The paper is organized as follows. We present in § 2 the data and the independent detection of absorption systems and star-forming galaxies. We then combine those detections in order to identify possible galaxy counterparts to the absorbers. In § 3 we focus on constraining covering fractions of C IV and Mg II, we present our results in § 4 and our conclusions in § 5. Throughout, we use a 737 cosmology ($H_0 = 70$ km s^{-1} Mpc^{-1}, $\Omega_m = 0.3$, and $\Omega_\Lambda = 0.7$) and a Chabrier (2003) stellar Initial Mass Function (IMF). All wavelengths and redshifts are in vacuum and are corrected to a heliocentric velocity standard. All distances are physical. All stated errors are 1σ, unless otherwise noted.

2 MUSE AND UVES OBSERVATIONS

The data we use in this study are part of a MUSE GTO program aiming to study gas flows around galaxies using background quasars. This MusE GAs FLOw and Wind (MEGAFLOW) program combines MUSE (Bacon et al. 2010) and UVES (Dekker et al. 2000) observations of 22 quasar fields and is described in Schroetter et al. (2016); Zabl et al. (2019); Schroetter et al. (2019). The quasar fields were selected based on the presence of at least 3 strong ($W_r^{\lambda 2796} > 0.5$–0.8Å) Mg II absorption in SDSS spectra and observed with MUSE with on average 3 hours of exposure time each. The observations and data reduction are described in Schroetter et al. (2016); Zabl et al. (2019).

For each field, UVES follow up observations of the quasar have been carried out. In this section, we present two individual types of detections: the first is the detection of [O II] emitters throughout all the 22 MUSE fields, the second is the detection of C IV and Mg II absorption systems in the UVES spectra. We then combine those two samples in order to search for absorber counterparts[1].

2.1 Galaxy detection in all MUSE fields from $z \geq 1.0$

In order to find star-forming galaxies potentially associated with C IV or Mg II absorbers, we blindly search for [O II] emitters in our MUSE fields, independently of any absorption systems. The MUSE wavelength range spans from ≈4700 to ≈9300 Å, at a spectral resolution of R≈ 2000 (or 150 km s^{-1}). This wavelength range allows the detection of [O II] emitters from redshifts $0.3 \leq z \leq 1.5$. UVES, on the other hand, allows for C IV absorption detection for redshift $z > 1.0$ with a spectral resolution of R≈ 38000[2]. In order to ensure overlapping redshift ranges between C IV and Mg II in UVES quasar spectra, we visually searched for [O II] emitters with redshifts 1.0–1.5 in the MUSE data, i.e in the 7400–9300 Å wavelength range. For this, we used narrow band images with the continuum subtracted throughout the cube wavelength range. In the 22 MEGAFLOW fields, we found 215 [O II] emitters and visually inspected each galaxy, making sure the [O II] emission doublet was clearly identified. In a forthcoming paper (Bouché et al. in prep.), we will characterize and present the detection completeness for the MEGAFLOW survey using a combination of automatic and visual inspection sources detection. Preliminary results based on inserting fake [O II] emitters with realistic sizes and kinematic properties give a 50% completeness level at $\approx 8.0 \times 10^{-18}$ erg s^{-1} cm^{-2} (corresponding to an SFR of ≈ 0.3 M$_\odot$ yr^{-1}at $z = 1.0$) for a typical depth of 3 hr in the red part of the MUSE wavelength range.

2.2 C IV and Mg II absorption systems

Using the MEGAFLOW UVES quasar spectra, we search for C IV and Mg II systems down to a rest-frame equivalent width (REW) W_r of 0.05Å at $z = 1$–1.5 , i.e. in the redshift range where both C IV and Mg II are covered by UVES and where [O II] can be detected in the MUSE wavelength range. The detection limit for each field is based on the signal to noise ratio and we find an overall equivalent width limit EW$_{\rm lim}$ ≈0.1 Å for both C IV and Mg II in the observed frame. Since all the absorption systems have $z > 1$, the rest EW$_{\rm lim}$ is thus divided by 1+z, leading to REW$_{\rm lim}$=0.05 Å. Examples of absorption and emission systems are shown in Figure 2. This Figure shows a selected sample of C IV, Mg II and [O II] systems detected at high, medium and low SNR. We emphasize here that each panel of this Figure is an independent system (different field, redshift or position).

We visually search all the 22 QSO's UVES spectra for C IV systems. Two of the authors performed this search independently

[1] We emphasize the fact that we do not use the final data reduction of MEGAFLOW data set but the same data as used in Schroetter et al. (2019) and Zabl et al. (2019).

[2] With a slit width of 1.2″ and a CCD readout with 2x2 binning. UVES observation settings and data quality are detailed in Zabl et al. (2019) and Schroetter et al. (2019).

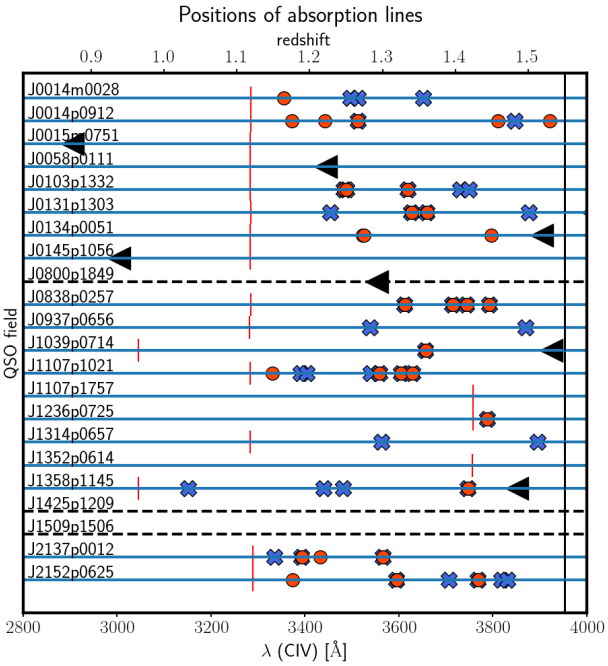

Figure 1. Position of C IV absorption systems for each MEGAFLOW field for which such systems are detected. The blue crosses represent the position of C IV absorption system. The top x axis represents the corresponding redshift. The red vertical lines represents the UVES lowest wavelength coverage and the black dashed vertical line the $z = 1.55$ redshift limit. The 3 horizontal black dashed lines are the fields for which the lowest UVES wavelength is above 4000 Å where C IV is not covered at $z \approx$1-1.5. The red circles show Mg II detections. The left black triangles show the quasar redshift positions. No left black triangles shown means that the quasar redshift is larger than 1.5.

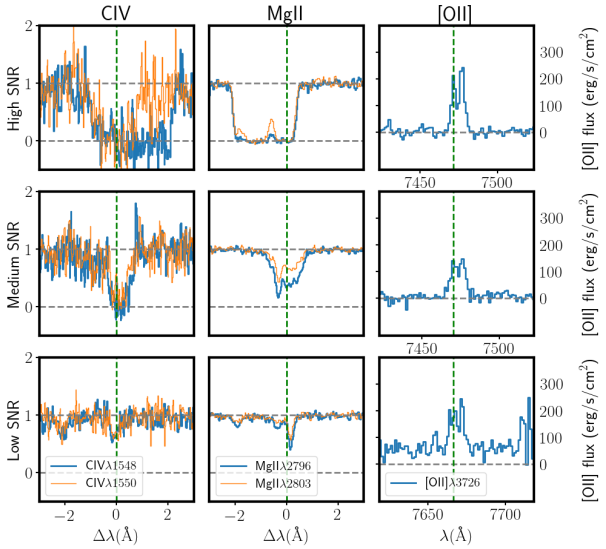

Figure 2. Examples of C IV (left) and Mg II (middle) absorption systems as well as [O II] (right) emission for high, medium and low Signal to Noise Ratio (SNR) in the top, middle and bottom rows, respectively. Each system is independent and were chosen arbitrary for example purpose.

and cross-checked the findings. In short, what we call a "confident C IV system" is a system having clear C IV($\lambda\lambda$ 1548, 1550) absorption. Both doublet components must have the same overall shape. No specific doublet ratio was required. Figure 1 shows the redshifts of all the C IV systems for each quasar sight-line. It is worth mentioning that for UVES fields which cover C IV and Mg II at redshift between 1.0 and 1.5, the spectral coverage is continuous.

In the 22 UVES spectra, we find a total of 41 C IV absorption systems with redshifts between 1.0 and 1.5, for which we also have Mg II coverage. Out of the 22 quasar fields, we only find C IV absorption systems in 13 of them. The 9 remaining fields either do not have UVES wavelength coverage (for 6 of them) or the quasars have lower redshift than 1.5 (for 3 of them). It is worth mentioning that within our selected wavelength coverage from redshifts 1 to 1.5 (from $\approx$ 3100 Å to $\approx$ 4000 Å), our UVES data do not have any spectral gap.

For those 41 C IV absorption systems, we also search for Mg II absorption lines. We find that out of the 41 C IV systems, 20 have Mg II absorption (see blue and hatched systems in Figure 3). We emphasize the fact that the MEGAFLOW survey was built based on Mg II absorption lines detected in quasar spectra from SDSS. Hence, we keep in mind that the numbers we give in this paper may be biased towards more Mg II absorption systems and that the MEGAFLOW selection may also increase the number of expected C IV systems. However, since this survey has the advantage of having high-resolution quasar spectra for each of the MUSE fields, we begin with this biased sample before building larger ones.

In order to complete our analysis and for the purpose of the covering fraction study later in this paper, we also search for all Mg II absorption systems in each of our UVES data, regardless of the presence of C IV absorbers. We first search for any Mg II absorption system with redshift between 1.0 and 1.5. Then, we reject the ones for which we cannot observe C IV absorption due to UVES wavelength coverage. In total, we find 52 Mg II systems. With the restriction cited above, we end up with 32[3] systems for which C IV absorption can be detected. The distribution of REW for all the Mg II systems is represented in Figure 4. Comparing the REW distribution of systems which have only C IV and the ones with the presence of Mg II (hashed histogram on Figure 4), we find that we are in good agreement with the study of Steidel & Sargent (1992) where they find that C IV-only systems are peaked towards lower REW. This difference could come from the fact that C IV may be more diffuse than Mg II around galaxies.

For simplicity, we choose to present a table summarizing all the different absorption systems for which both absorption lines (C IV and Mg II) can be detected. Table 1 shows the absorption system redshift with the corresponding REW of C IV($\lambda\lambda$1548, 1550) and Mg II($\lambda\lambda$2796, 2803) (if detected) absorption lines. We note that each C IV or Mg II doublet is resolved and each corresponding limit was applied to each individual doublet members.

Having independently detected the absorption systems in UVES spectra and the [O II] emitters in MUSE, we next try to match galaxies to absorption systems.

2.3 Absorber counterparts

We now look for galaxies which possibly correspond to the C IV absorption systems. For each detected galaxy, we measure the

[3] Those 32 systems are covering possible C IV absorption, this does not mean that we actually detect them. Indeed, we only detect 20 C IV systems out of those 32.

Table 1. Absorption system properties

Field name (1)	z_{abs} (2)	$W_r^{\lambda1548}$ (3)	$W_r^{\lambda1550}$ (4)	$W_r^{\lambda2796}$ (5)	$W_r^{\lambda2802}$ (6)
J0014m0028	1.16444	≤ 0.05	≤ 0.05	0.3251	0.2721
···	1.25638	0.6108	0.3913	≤ 0.05	≤ 0.05
···	1.35566	0.0655	0.0762	≤ 0.05	≤ 0.05
J0014p0912	1.17550	≤ 0.05	≤ 0.05	0.9277	0.8453
···	1.22115	≤ 0.05	≤ 0.05	1.2521	0.9717
···	1.26575	1.5459	0.9266	0.3772	0.1909
···	1.45844	≤ 0.05	≤ 0.05	0.2831	0.1541
···	1.48212	0.1778	0.3613	≤ 0.05	≤ 0.05
J0103p1332	1.24646	0.5493	0.5053	0.2369	0.1577
···	1.25029	0.5005	0.1065	≤ 0.05	≤ 0.05
···	1.33451	0.4467	0.3516	0.3347	0.2231
···	1.34053	≤ 0.05	≤ 0.05	0.1687	0.1107
···	1.36112	≤ 0.05	≤ 0.05	0.3727	0.2989
···	1.40648	0.3491	0.2141	≤ 0.05	≤ 0.05
···	1.41847	0.9428	0.6973	≤ 0.05	≤ 0.05
J0131p1303	1.22845	0.2819	0.2384	≤ 0.05	≤ 0.05
···	1.33945	0.7591	0.5660	0.1567	0.1024
···	1.36075	0.3734	0.3213	0.3582	0.2862
···	1.50130	0.0947	0.0695	≤ 0.05	≤ 0.05
J0134p0051	1.27246	≤ 0.05	≤ 0.05	0.3312	0.2847
···	1.27411	≤ 0.05	≤ 0.05	0.3500	0.2266
···	1.44917	≤ 0.05	≤ 0.05	0.4287	0.2362
J0838p0257	1.33042	1.4164	1.1392	1.5306	1.2020
···	1.39601	0.5442	0.5272	0.0598	0.0228
···	1.41490	0.7320	0.3133	0.8686	0.6654
···	1.44629	1.4876	1.2233	0.7595	0.5980
J0937p0656	1.28260	1.0395	0.7001	≤ 0.05	≤ 0.05
···	1.49647	1.0355	1.0112	≤ 0.05	≤ 0.05
J1039p0714	1.35888	1.1127	1.0100	2.4970	2.2989
J1107p1021	1.14907	≤ 0.05	≤ 0.05	0.7981	0.515
···	1.18750	0.2123	0.1948	≤ 0.05	≤ 0.05
···	1.19557	0.4752	0.1473	≤ 0.05	≤ 0.05
···	1.28363	0.2810	0.1408	≤ 0.05	≤ 0.05
···	1.29562	2.1644	1.9257	0.5323	0.2984
···	1.32523	1.6618	1.4281	2.7651	2.6038
···	1.34105	1.2897	1.0869	0.1009	0.0524
J1236p0725	1.44338	0.4736	0.3960	1.7089	1.5374
J1314p0657	1.29867	0.2399	0.1287	≤ 0.05	≤ 0.05
···	1.51345	0.1353	0.1080	≤ 0.05	≤ 0.05
J1358p1145	1.03320	1.1543	0.9007	≤ 0.05	≤ 0.05
···	1.21902	0.1625	0.1520	≤ 0.05	≤ 0.05
···	1.24627	0.0615	0.0350	≤ 0.05	≤ 0.05
···	1.41709	0.9830	0.7056	2.5651	2.3938
J2137p0012	1.15191	0.2559	0.1254	≤ 0.05	≤ 0.05
···	1.18860	0.6404	0.4889	0.2686	0.1671
···	1.21472	≤ 0.05	≤ 0.05	1.1219	1.0573
···	1.30023	0.4736	0.1542	0.0731	0.0590
J2152p0625	1.17651	≤ 0.05	≤ 0.05	0.496	0.3924
···	1.31870	1.3851	0.9527	1.3841	1.1038
···	1.39149	0.8075	0.7151	0.0123	0.0234
···	1.43101	1.0550	0.9595	0.9884	≤ 0.05
···	1.46349	0.4458	0.1634	≤ 0.05	≤ 0.05
···	1.47132	0.5880	0.4002	≤ 0.05	≤ 0.05

1: Field name; 2: Absorption system redshift; 3: C IV (λ1548) REW (Å); 4: C IV (λ1550) REW (Å); 5: Mg II (λ2796) REW (Å); 6: Mg II (λ2802) REW (Å). Typical EW 1-σ errors are 0.01 Å.

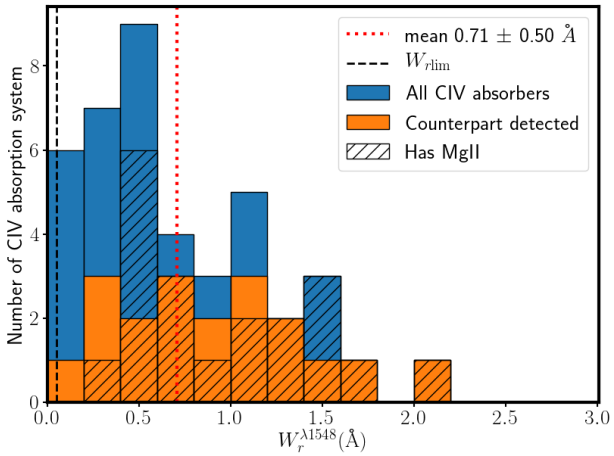

Figure 3. Histogram showing number of C IV absorption systems as a function of their REW for all the C IV absorbers (in blue), the ones with galaxy counterparts detected (in orange) and the number of absorbers for which we also detect Mg II absorption lines (hatched). The REW detection limit is shown by the black dashed vertical line

velocity difference[4] between C IV absorption and [O II] emission. Our criterion is that a galaxy is considered to be a counterpart if $|\Delta v| < 500$ km s^{-1}.[5] With this criterion, we find 39 counterpart galaxies for 19 C IV absorption systems, out to 250 kpc from the quasar. Out of those 19 systems, 15 (≈ 80%) have Mg II absorption lines.

One of the most interesting results is that out of all the 21 systems with only C IV absorption detected (not Mg II), we detect counterparts for only 4 systems. This means that we do not detect any counterpart for 80% of those "C IV only" systems. This result suggests that the C IV gas is probably located in the IGM rather than in the CGM or that C IV is associated with galaxies with lower SFR than Mg II. As already argued by Rahmani et al. (2018), a system having both C IV and Mg II absorption lines appears to have a higher chance of a counterpart detection, compared to a system with only C IV absorption. Here we can confirm this statement as 80% of our systems for which we find at least 1 counterpart have both C IV and Mg II absorption lines.

Using the same criterion to identify counterparts of the 52 detected Mg II systems, we find 72 counterparts for 33 of them (≈ 63%), within 250 kpc from the quasar[6]. We note that 21 of those 33 systems were part of the original MEGAFLOW selection.

3 MEASURING COVERING FRACTIONS

With our sample of [O II] galaxies, we can now have a look at the covering fractions of C IV and Mg II for redshifts $1.0 < z < 1.5$. The covering fraction is defined (e.g. Bordoloi et al. 2014)

$$C_f(r) \equiv \frac{N_{W_r > W_{r,\lim}}(r)}{N_{\rm tot}(r)} \quad (1)$$

[4] The velocity difference between the absorber redshift and the galaxy systemic redshift

[5] We also search for systems with $\Delta v < 1000$ km s^{-1} but found no more associations

[6] We emphasize the fact here that this is the counterpart detection rate for $z > 1$ galaxies in MEGAFLOW, compared to the ≈ 80% detection of the whole survey for redshifts $0.4 < z < 1.5$

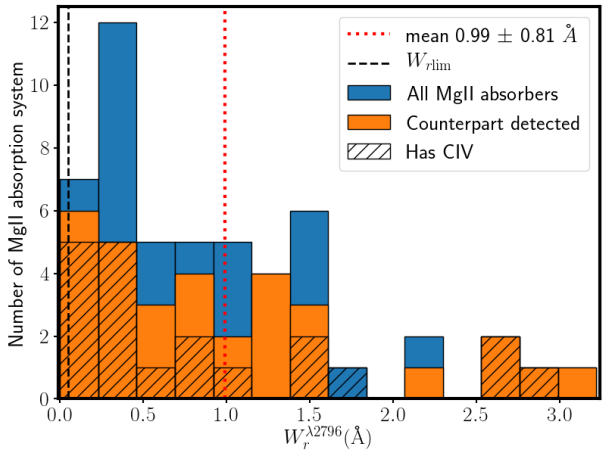

Figure 4. $W_r^{\lambda 2796}$ distribution for all detected Mg II absorption systems. It is worth mentioning that the mean value for absorbers originally in MEGAFLOW selection is $< W_r^{\lambda 2796} >= 1.41$ Å.

where $N_{W_r > W_{\rm r,lim}}$ is the fraction of sight-lines at a given impact parameter with a W_r above a limit $W_{\rm r,lim}$.

While $C_f(r)$ is typically determined in radial bins, we use here a novel unbinned approach using logistic regression. As discussed in Hosmer & Lemeshow (2000), a logistic regression (LR) is a statistical technique commonly used to examine the possible relationship between a dichotomous variable (here whether the galaxies absorption are detected in the quasar spectra) and independent variables (X_n, such as impact parameter, redshift, etc.) [7]. In general, the probability p for a galaxy to be detected (i.e., $Y = 1$) can be described by any continuous function $p = L(t)$. Here, we use a logistic function for the probability p to detect a galaxy, which yields a continuous transition of p from 0 to 1:

$$p(Y = 1) = \frac{1}{1 + \exp(-t)} \equiv L(t) \quad (2)$$

where t is usually taken to be a linear combination of the independent variables, X_n, i.e., $t = \alpha + \beta_1 X_1 + \cdots + \beta_n X_n$.[8]

Then, the probability to have a detection is given by the Bernoulli probability distribution Bern(p), since the observables are dichotomous, with values at 0 or 1, for undetected and detected systems, respectively. In summary, the LR model is

$$t = f(X_i; \theta) \quad (3)$$

$$p = L(t) \quad (4)$$

$$O \sim \mathrm{Bern}(p) \quad (5)$$

where X_i are the independent variables, θ are the model parameters, and O are the simulated observables which are compared to the observed data.

We chose a linear model f to be a simple linear function of impact parameter b,

$$f(b; \theta) = A\,(\log b - \mathrm{ZP}) \quad (6)$$

where A describes the slope of the covering fraction and ZP the zero-point at 50% covering fraction $f_c = 0.5$, since $L(0) = 0.5$. One could add a redshift dependent zero-point

$$f(b, z; \theta) = A\,(\log b - \mathrm{ZP}(z)) \quad (7)$$

where $\mathrm{ZP}(z) = B \log(1 + z) + C$. This second model is discussed/shown in § 4.

We use a Markov Chain Monte Carlo (MCMC) algorithm to estimate the best fitting parameters $\hat{\theta}$ for our model. Because traditional MCMC algorithms are somewhat sensitive to the step size and the desired number of steps, in what follows we use the No-U Turn Sampler (NUTS) of Hoffman & Gelman (2014) implemented in Pymc3 (Salvatier et al. 2016), a self-tuning variant of Hamiltonian Monte Carlo (HMC). We typically use 2 MCMC chains per run and 4,500 iterations per chain.

We stress that the purpose of this exercise is to demonstrate the viability of our new technique for determining the covering fractions of metal lines in the regime of small number statistics.

4 RESULTS

4.1 Mg II covering fraction

The distribution of Mg II REWs for all detected absorbers is shown in Fig. 4. The Mg II systems have REWs of [0.1-2.5Å] with a mean of $W_r^{2796} = 0.99 \pm 0.8$Å. As discussed in Appendix A2, the mean REW $< W_r^{\lambda 2796} >$ of our sample is biased towards high $W_r^{\lambda 2796}$ compared to random field Mg II absorbers due to the MEGAFLOW survey selection criteria (§ 2).

Fig. 5(bottom) shows the Mg II covering fraction f_c as a function of impact parameter b, where the filled squares with Poisson error bars (1σ) show the binned data. The solid line represents a logistic fit to the unbinned data with its 95% confidence interval (grey area) derived from the Markov chain. The 50% covering fraction $f_c(50\%)$ occurs at $\log b/\mathrm{kpc} = 1.66 \pm 0.15$ (2σ), corresponding to 46^{+18}_{-13} kpc. Our results are broadly in agreement with the study of Nielsen et al. (2013a) (grey triangles) which used a sample of 182 galaxies towards 134 quasar sight-lines over a wide redshift range of $0.07 \leq z \leq 1.12$. Fig. 5(top) shows the redshift evolution determined from our model Eq. 7. The solid line shows that $f_c(50\%)$ evolves as $(1 + z)^a$ with $a = 1.7^{+2.5}_{-2.7}$ (2σ), i.e. consistent with no redshift evolution. This figure shows the benefit of our parametric fit to the detected/undetected systems.

Among literature results of Mg II covering fractions, Lan (2020) stands out with a sample of 15,000 Mg II-galaxy pairs in SDSS with $W_r^{2796} > 0.4$ Å (albeit with photometric redshifts). Their f_c as a function of radius (redshift) is shown with the dotted line in the bottom (top) panel of Fig. 5, respectively. In spite of our much smaller sample, our results are in good agreement with theirs. The dotted line in Fig. 5(bottom) from Lan (2020) has been calculated for absorbers with $W_r^{2796} \geq 1$Å [9], at $z = 1.2$, for star-forming galaxies with $\log(M_\star/M_\odot) = 10.0$ assuming a $R_{\rm vir} \approx 200 - 250$ kpc from their Eqs 7–9. The solid line in Fig. 5(top) has been calculated by solving numerically for the redshift evolution in Lan (2020).

It is interesting to compare the halo mass for Mg II absorbers corresponding to $R_{\rm vir} \approx 200 - 250$ kpc, namely $\log M_{\rm h}/\mathrm{M}_\odot \approx 12.6$, to the mass scale obtained by Bouché et al. (2006) from a clustering analysis of 2,500 $z = 0.5$ absorbers (see also Gauthier et al. 2009; Lundgren et al. 2009, 2011): $\log M_{\rm h}/\mathrm{M}_\odot \approx 12.5 \pm 0.4$ for their absorbers with $0.3 < W_r^{2796} < 1.15$. The covering fraction could also be weakly dependent on stellar mass (e.g. Chen et al. 2010; Nielsen

[7] For an application of the technique, see Bouché & McConway (2019).
[8] This assumes that all variables are independent of one another, but covariance terms can be included.

[9] Lan (2020) does not provide a fit for $W_r^{2796} > 0.4$Å absorbers, but the equivalent width dependence seems small compared to the other parameters.

Fitted parameters	A [95%]	B [95%]	C [95%]
Mg II	−4.2 [-5.7;-2.9]	1.0 [0.2; 1.9]	2.0 [-0.7; 4.3]
C IV	−2.8 [-4.5;-1.2]	1.6 [0.3;2.8]	-0.7 [-4.7;3.2]

Table 2. Fitted parameters for f_c for Mg II and C IV in relation to Eq. 7 along with their 95% confidence interval.

et al. 2013a; Lan 2020), but we reserve such an analysis to a forthcoming paper on the full MEGAFLOW sample. Nonetheless, these results are a demonstration of the power of our fitting technique on unbinned data.

4.2 C IV covering fraction

From a total of 215 [O II] emitters in the MUSE data with redshift >1.0, after looking at the redshift differences between each emitter and C IV absorption systems, we found 39 galaxy counterparts corresponding to 19 C IV absorption systems. Incidentally, 80% (15 out of 19) of those systems have detectable Mg II absorption lines as well [10].

Fig. 6 shows the covering fraction as a function of impact parameter, where the filled squares with Poisson error bars (1σ) show the binned data and the solid line represents logistic fit to the unbinned data (red squares). The 50% covering fraction occurs at $\log b/\mathrm{kpc} = 1.55 \pm 0.38$ (2σ), i.e. ≈30 kpc.

We can compare our C IV covering fraction with the study of Bordoloi et al. (2014), which used a sample of 43 low-mass $z \leq 0.1$ galaxies using background quasars observed with COS. In their study, they find that C IV is detected up to 100 kpc from the host galaxy and that the column density of this gas falls off as a power law. Our f_c(C IV) appears to be in good agreement with their study.

Comparing f_c(Mg II) and f_c(C IV) in Figs. 5-6, the radius corresponding to a covering fraction of 50% is similar for C IV and Mg II at 30-45 kpc given the current sample, with a hint that f_c(C IV) is shallower than f_c(Mg II). The similarity between f_c(C IV) and f_c(Mg II) is be in agreement with studies of C IV and Mg II covering fractions in quasar environments (Landoni et al. 2016). Since 80% of C IV systems have detectable Mg II the covering fraction for systems with both Mg II and C IV is very similar. The fitted parameters for the covering fractions using Eq. 7 are listed in Table 2.

5 DISCUSSION AND CONCLUSION

This study is divided into two parts: (i) the independent detection of absorption systems in MEGAFLOW UVES and [O II] emitters in MEGAFLOW MUSE with the identification of galaxy counterparts to the absorbers; (ii) measurement of the covering fractions of C IV and Mg II.

Using the MEGAFLOW UVES quasar spectra, we searched for C IV, Mg II systems at z = 1–1.5, i.e. in the redshift range where both C IV and Mg II are covered by UVES and where [O II] could be detected in the MUSE wavelength coverage, down to a rest-frame equivalent width of 0.05Å. We detect a total of 51 Mg II absorption systems and 41 C IV absorption systems independently. 50%

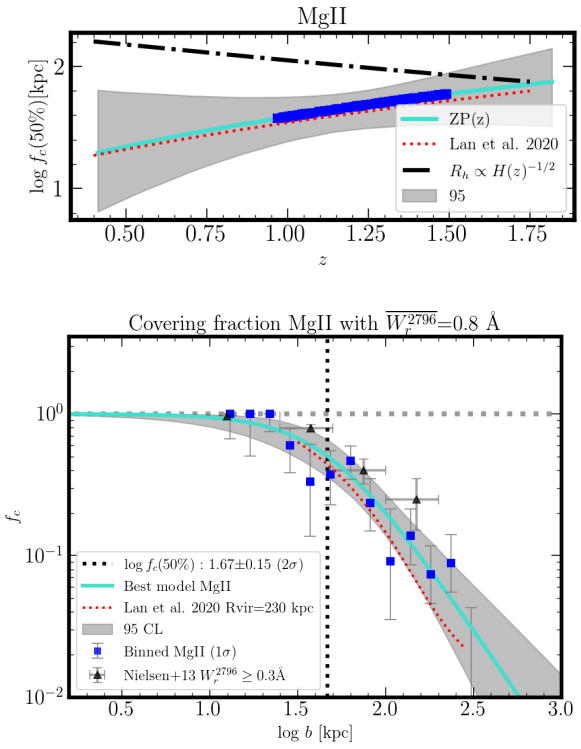

Figure 5. *Bottom:* Mg II covering fraction f_c as a function of impact parameter b. The solid blue squares show the binned data with 1σ **Wilson intervals**. The error bars are shown only with at least 2 galaxies contributing. The logistic fit Eq. 6 to the *unbinned* data is shown with the solid blue line and its 2σ confidence region is shown by the shaded region. The 50% covering fraction is found to be at $\log b/\mathrm{kpc} = 1.66 \pm 0.15$ or $b \simeq 45$ kpc. The dotted red line represents the fit found by Lan (2020) for z = 1.2, $\log(M_\star/\mathrm{M}_\odot) = 10$ and $R_{\mathrm{vir}} = 250$ kpc. The triangles represent the Nielsen et al. (2013a) results. *Top:* The redshift evolution of the 50% covering fraction with the 2σ predictive interval shown in grey. With our sample, the redshift evolution is in good agreement with that of Lan (2020) (red solid line) but also consistent with no evolution.

and 60% of the 41 C IV and 32 Mg II systems[11], respectively, have absorption by both ions.

Using the 22 MEGAFLOW MUSE fields, we searched for [O II] emitters at redshift z =1.0–1.5 and found a total of 215 emitters down to a flux limit of ≈ 10^{-17} erg s^{-1} cm^{-2} (Schroetter et al. 2016, 2019; Zabl et al. 2019). For each of these 215 [O II] galaxies, we searched in our catalog of C IV systems with REW > 0.05 Å for matches within 500 km s^{-1} and b < 250 kpc. We found 39 galaxies associated with 19 C IV systems. For each galaxy, we also searched for corresponding Mg II systems and found 72 galaxies associated with 33 Mg II systems, of which 21 **galaxies** were in the original MEGAFLOW selection. 80% of the systems for which we detect at least one galaxy counterpart have both C IV and Mg II absorption lines. We also highlight that 80% of the 'only C IV' systems do not appear to have any galaxy counterpart in any MUSE field. This suggests that C IV-only gas is more likely to be part of the IGM, i.e. beyond 250 kpc rather than of the CGM, or that C IV is preferentially associated with very low mass galaxies.

[10] MEGAFLOW was not designed around C IV absorption system, this 80% might be indirectly biased by our Mg II selection.

[11] The 32 Mg II systems are the ones for which C IV can possibly be detected

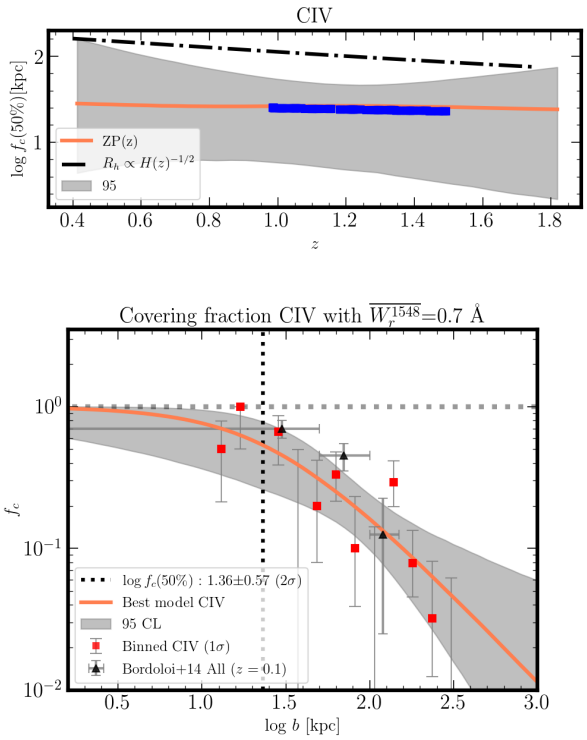

Figure 6. *Bottom:* C IV covering fraction f_c as a function of impact parameter b. The solid red squares show the binned data with 1σ **Wilson intervals**. The error bars are shown only with at least 2 galaxies contributing. The logistic fit Eq. 6 to the *unbinned* data is shown with the solid orange line and its 95% (2σ) confidence region is shown by the shaded region. The black triangles represent the Bordoloi et al. (2014) $z = 0$ results. The 50% covering fraction is found to be at $\log b/\mathrm{kpc} = 1.38 \pm 0.48$ or $b \simeq 30$ kpc. *Top*: The redshift evolution of the 50% covering fraction with the 2σ predictive interval shown in grey.

Then, using the closest associated galaxies in our small sample of 19 (30) C IV (Mg II) absorber-galaxy pairs, we find that the C IV and Mg II covering fractions are similar with $f_c(50\%) \approx 30$–45 kpc. In addition, the covering fraction f_c with radius for strong Mg II absorbers (with mean $W_r \simeq 1$Å) follows closely the results of Lan (2020) who used 15,000 pairs. Our sample is too small to study the redshift evolution with confidence, but our results follow the trend expected from the Lan (2020) study. This Mg II redshift evolution suggests that the Mg II gas/halo is becoming smaller with time at a given (halo) mass. This evolution also suggests low escape fractions for the Mg II gas, pointing towards the implication for the recycling of this gas. Whereas the warm C IV halo covering fraction evolution is consistent with no redshift evolution, suggesting a more stable halo.

The 40 kpc covering fraction points to a physical picture where Mg II and C IV are associated to individual "massive"/$L_\star$/sub-$L_\star$ galaxies for large REWs. With the final MEGAFLOW survey and upcoming larger surveys , we will be able to address this redshift evolution and the potential dependence of covering fraction on azimuthal angle and/or EWs, thus yielding a better understanding of the CGM.

In conclusion, we showed, with the MEGAFLOW survey, our ability to constrain the covering fractions of absorption lines (such as Mg II, C IV) in the regime of low-number statistics using a Bayesian logistic regression (§ 3). This approach allows one to fit a parametric model directly to unbinned binary data (1/0) where 1 represents an absorption detection and 0 its absence. The advantage of our method is that it does not suffer from the limitations caused by small number statistics inherent when using binned data.

ACKNOWLEDGMENTS

We thank the referee for useful comments which led to an improved paper. This work has been carried out thanks to the support of the ANR 3DGasFlows (ANR-17-CE31-0017), the OCEVU Labex (ANR-11-LABX-0060).

Software: This work made use of the following open-source software: Numpy (Van Der Walt et al. 2011), Scipy (Jones et al. 2001), Matplotlib (Hunter 2007), and Pymc3 (Salvatier et al. 2016). SM is supported by the Alexander von Humboldt-Stiftung via the Experienced Researchers fellowship.

APPENDIX A:

References

Bacon, R., Accardo, M., Adjali, L., et al. 2010, in Society of Photo-Optical Instrumentation Engineers (SPIE) Conference Series, Vol. 7735, Society of Photo-Optical Instrumentation Engineers (SPIE) Conference Series, 8
Bordoloi, R., Tumlinson, J., Werk, J. K., et al. 2014, ApJ, 796, 136
Bouché, N. & McConway, K. 2019, Bioelectromagnetics, 40, 539
Bouché, N., Murphy, M. T., Péroux, C., Csabai, I., & Wild, V. 2006, MNRAS, 371, 495
Chabrier, G. 2003, PASP, 115, 763
Chen, H., Wild, V., Tinker, J. L., et al. 2010, ApJ, 724, L176
Chen, H.-W., Lanzetta, K. M., & Webb, J. K. 2001, ApJ, 556, 158
Churchill, C. W., Rigby, J. R., Charlton, J. C., & Vogt, S. S. 1999, ApJS, 120, 51
Dekker, H., D'Odorico, S., Kaufer, A., Delabre, B., & Kotzlowski, H. 2000, in Proc. SPIE, Vol. 4008, Optical and IR Telescope Instrumentation and Detectors, ed. M. Iye & A. F. Moorwood, 534–545
Du, X., Shapley, A. E., Martin, C. L., & Coil, A. L. 2016, ApJ, 829, 64
Fox, A. & Richter, P. 2016, A&A, 588, A94
Fox, A. J., Ledoux, C., Petitjean, P., & Srianand, R. 2007, A&A, 473, 791
Gauthier, J., Chen, H., & Tinker, J. L. 2009, ApJ, 702, 50
Hoffman, M. D. & Gelman, A. 2014, Journal of Machine Learning Research, 15, 1593
Hosmer, D. W. & Lemeshow, S. 2000, Applied logistic regression (John Wiley and Sons)
Hunter, J. D. 2007, Computing in Science and Engineering
Jones, E., Oliphant, T., Peterson, P., et al. 2001
Lan, T.-W. 2020, ApJ, 897, 97
Landoni, M., Falomo, R., Treves, A., Scarpa, R., & Farina, E. P. 2016, MNRAS, 457, 267
Lundgren, B. F., Brunner, R. J., York, D. G., et al. 2009, ApJ, 698, 819
Lundgren, B. F., Wake, D. A., Padmanabhan, N., Coil, A., & York, D. G. 2011, MNRAS, 417, 304
Narayanan, A., Misawa, T., Charlton, J. C., & Kim, T.-S. 2007, ApJ, 660, 1093
Nestor, D. B., Turnshek, D. A., & Rao, S. M. 2005, ApJ, 628, 637
Nielsen, N. M., Churchill, C. W., & Kacprzak, G. G. 2013a, ApJ, 776, 115
Nielsen, N. M., Churchill, C. W., Kacprzak, G. G., & Murphy, M. T. 2013b, ApJ, 776, 114
Prochaska, J. X., Lau, M. W., & Hennawi, J. F. 2014, ApJ, 796, 140
Rahmani, H., Péroux, C., Schroetter, I., et al. 2018, MNRAS, 480, 5046
Rauch, M., Sargent, W. L. W., & Barlow, T. A. 2001, ApJ, 554, 823
Salvatier, J., Wiecki, T. V., & Fonnesbeck, C. 2016, PeerJ Comput. Sci., 2, e55
Schaye, J., Aguirre, A., Kim, T., et al. 2003, ApJ, 596, 768

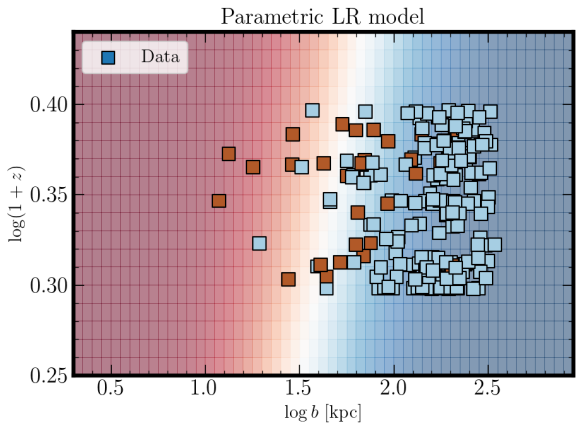

Figure A1. Two dimensional covering fraction of Mg II as a function of impact parameter $\log b$ and redshift $\log 1 + z$. The unbinned data is shown as blue (red) squares representing the undetected (detected) systems, respectively. The covering fraction from the logistic fit is represented by the background color with low (high) covering fractions represented as blue (red) respectively.

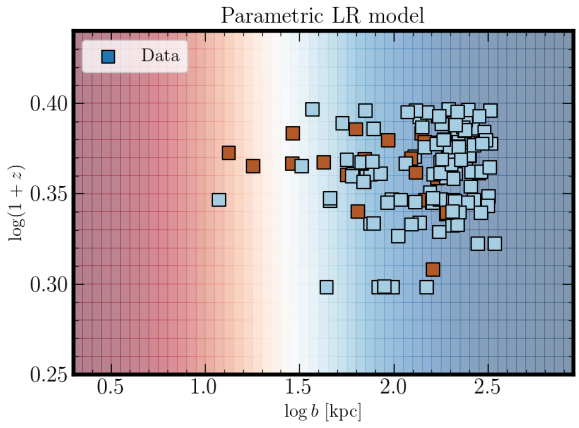

Figure A2. Redshift as a function of impact parameter for all the detected galaxies (squares). Galaxies corresponding to a C IV absorption system are shown in brown. The background color represent the covering fraction of C IV.

Schaye, J., Crain, R. A., Bower, R. G., et al. 2015, MNRAS, 446, 521
Schroetter, I., Bouché, N., Wendt, M., et al. 2016, ApJ, 833, 39
Schroetter, I., Bouché, N. F., Zabl, J., et al. 2019, MNRAS, 2451
Steidel, C. C. & Sargent, W. L. W. 1992, ApJS, 80, 1
Tumlinson, J., Peeples, M. S., & Werk, J. K. 2017, ARA&A, 55, 389
Turner, M. L., Schaye, J., Crain, R. A., et al. 2017, MNRAS, 471, 690
Turner, M. L., Schaye, J., Steidel, C. C., Rudie, G. C., & Strom, A. L. 2014, MNRAS, 445, 794
Van Der Walt, S., Colbert, S. C., & Varoquaux, G. 2011, Computing in Science and Engineering, 13, 22
Zabl, J., Bouché, N. F., Schroetter, I., et al. 2020, MNRAS, 492, 4576
Zabl, J., Bouché, N. F., Schroetter, I., et al. 2019, MNRAS, 485, 1961

A1 Possible bias towards strong absorbers

In Figure A3, we compare the distribution of $W_r^{\lambda 2796}$ with literature samples. Our sample (blue circles) has an overabundance of strong absorbers compared to other Mg II surveys due to the MEGAFLOW

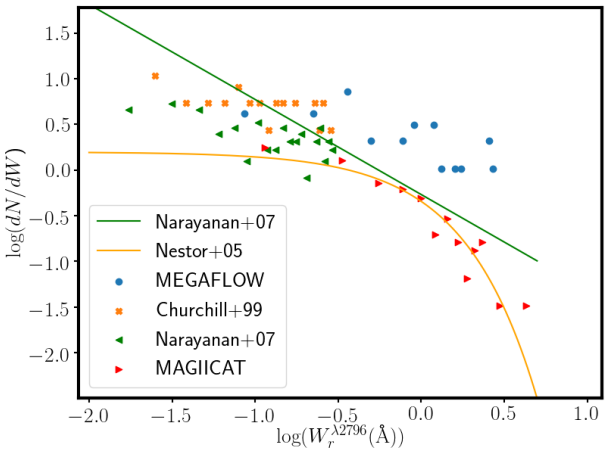

Figure A3. $W_r^{\lambda 2796}$ distribution of our absorption systems (blue circles) and from other studies. The green line represents the fit from Narayanan et al. (2007) and the orange curve the one from Nestor et al. (2005). The MAGIICAT points in red right triangles are from Nielsen et al. (2013b), the orange crosses from Churchill et al. (1999) and the left green triangles are from Narayanan et al. (2007).

selection of multiple strong Mg II absorbers in quasar spectra. However, the lower REW population ($\log(W_r^{\lambda 2796}) \leq -0.5$) of MEGAFLOW absorbers found in this study, which are not preselected, are in agreement with other studies.